



ALMA MATER STUDIORUM
UNIVERSITÀ DI BOLOGNA

ARCHIVIO ISTITUZIONALE
DELLA RICERCA

Alma Mater Studiorum Università di Bologna Archivio istituzionale della ricerca

Probability-density risk-maps for tourism during emergencies

This is the final peer-reviewed author's accepted manuscript (postprint) of the following publication:

Published Version:

Pantano, E. (2022). Probability-density risk-maps for tourism during emergencies. ANNALS OF TOURISM RESEARCH, 92, 1-6 [10.1016/j.annals.2021.103259].

Availability:

This version is available at: <https://hdl.handle.net/11585/841891> since: 2021-12-16

Published:

DOI: <http://doi.org/10.1016/j.annals.2021.103259>

Terms of use:

Some rights reserved. The terms and conditions for the reuse of this version of the manuscript are specified in the publishing policy. For all terms of use and more information see the publisher's website.

This item was downloaded from IRIS Università di Bologna (<https://cris.unibo.it/>).
When citing, please refer to the published version.

(Article begins on next page)

This is the final peer-reviewed accepted manuscript of:

Pantano, E., Scarpi, D., Vannucci, V., Bilotta, E., & Pantano, P. (2022). Probability-density risk-maps for tourism during emergencies. *Annals of Tourism Research*, 92(C).

The final published version is available online at:

<https://doi.org/10.1016/j.annals.2021.103259>

Rights / License:

The terms and conditions for the reuse of this version of the manuscript are specified in the publishing policy. For all terms of use and more information see the publisher's website.

This item was downloaded from IRIS Università di Bologna (<https://cris.unibo.it/>)

When citing, please refer to the published version.

1 **DYNAMIC RISK-MAPS FOR TOURISM DURING EMERGENCIES**

2

3 **1. Introduction**

4 Tourism locations can be subject to emergencies that negatively affect tourism as people are afraid
5 for their safety (Ritchie and Jiang 2019). Past studies have addressed the impact of risk perception
6 on travel behavior and decision-making (e.g., Zenker and Kock 2020). They found that the majority
7 of tourists is risk-adverse and over-estimates tourism-related risks (Wang et al. 2019). Thus, tourists
8 change travel intentions and behavior to avoid risks, for instance, deferring travel (Wiliams and
9 Balaz 2015). The COVID-19 pandemic provides a global example that is going on for several
10 months now (Karabulut et al., 2020), with multi-billion losses.

11 This paper shows how to develop extremely detailed dynamic probability-density maps that represent
12 an area's actual risk. They can help realign the risk perceptions of anyone visiting the region or
13 residing there, but might apply in particular to tourists, as these maps allow to plot risk-levels around
14 specific landmarks, like tourist attractions. Thus, they can contribute to containing the negative effects
15 of an emergency by helping tourists and policy-makers identify which attractions are safe to visit and
16 through which routes. As a consequence of implementing these maps, destinations can support
17 tourism even during an emergency without compromising people's health and safety, rather than
18 stopping tourisms tout-court. Such outcome could help both government and tourism managers
19 (Ritchie & Jiang, 2019).

20 In the following, we show how to develop a probability-density risk-map of COVID-19 contagion
21 for London. London was chosen as it is one of the main global destinations before the pandemic,
22 with approximately 16.38 million overseas tourists in 2019 alone (Statista 2020). We map the main
23 tourist attractions scattered across the city and each area's risk level, square-foot by square-foot.

24 Then, we provide examples of how prospective tourists react to the map.

25

26 **2. Dynamic probability-density risk-maps**

27 Since individuals are dynamic entities, we need to model their behavior considering their (probable)
28 movements in space, which impacts contact risk with infected/contagion.

29 First, we need to identify the mathematical function (f) characterizing our space (London). We call
30 S the space (London), and r the attractions. To place the attractions (r) on the map of the space (S),
31 we envision each attraction as a vector of two Real numbers, corresponding to its latitude and
32 longitude. Thus:

$$33 \quad f: S \rightarrow \mathbb{R}; r \in S \mapsto f(r) \in \mathbb{R} \quad (1)$$

34 In this application, we map attractions with at least 15,000 reviews on TripAdvisor (at the time of
35 data collection), which corresponds to the highest reviews rank. This led to the identification of 18
36 attractions, reported in Table 1.

37 Secondly, we define mathematically the probability of meeting an infected while visiting an
38 attraction:

$$39 \quad f(r) \geq 0 \forall r \in S \text{ and } \iint_S f(r) dr = 1 \quad (2).$$

40 London (S) is organized into 33 local authority districts (boroughs) (Σ). Formally: $\Sigma \subseteq S$. Hence,
41 the probability of meeting an infected in a specific borough is:

$$42 \quad P(\Sigma) = \iint_{\Sigma} f(r) dr,$$

43 Also, $f(r) = \lim_{\Sigma \rightarrow r} \frac{P(\Sigma)}{|\Sigma|}$, where $|\Sigma|$ is Lebesgue's measure of Σ (3).

44
45 Third, density correlates with contacting: the more infects in a place, the more likely contact becomes
46 (Bertacchini et al., 2020). Although other factors besides density could play a role (e.g., open vs.
47 closed spaces), density is considered the dominant factor to explain contagion probability (e.g.,
48 Castorina et al., 2020; Godio et al., 2020). Thus, the contact risk with an infect in borough Σ correlates
49 with the number of infects in that borough and rises contagion risk.

50 Because the data about the number of infected in each of the 33 boroughs of London (Σ_1 to Σ_{33}) are
51 cumulative and not homogeneous, we split the model for each borough. The total number of infects
52 (T) in the 33 boroughs are:

$$53 T = \{\Sigma_i, i = 1, 2, \dots, n : \Sigma_i \subset \Sigma, \cup \Sigma_i = S \text{ and } \Sigma_i \cap \Sigma_j = 0 \text{ if } i \neq j\} (4).$$

54

55 The UK Government publishes daily data (D) regarding the number of COVID-19 contagions (m_i)
56 in London's 33 boroughs: $D = \{(m_i, \Sigma_i), i = 1, 2, \dots, n\}$. Where $m_i \in \mathbb{N}$ is the number of infects in
57 any given borough Σ_i . The association between each borough Σ_i , the number of infects m_i and the
58 attractions r_{ij} in the borough is:

$$59 \Sigma_i \mapsto \{r_{ij} \in \Sigma_i | j = 1, 2, \dots, m_i\} (5).$$

60

61 Four, assuming a homogeneous distribution of the m_i infected persons of a borough, m_i can be
62 assumed to be distributed randomly. Thus, m_i follows a normal bivariate distribution with mean in
63 s_i , where s_i is the geo-localization associated with the specific borough Σ_i . Consequently, s_i
64 represents a point in the borough and can be interpreted as the smallest space unit, like the square
65 feet where one is standing. In other words, the map shows the probability density function of
66 meeting an infected for the whole of London, borough by borough, and the smallest fraction inside
67 each borough. This level of spatial detail is not only unprecedented, but also functional, as infected
68 might move around (unless hospitalized or quarantined).

69 Five, the probability of contacting an infected while visiting a tourist attraction in a borough, can be
70 evaluated through the probability function based on the Density Kernel Estimator Method (Botev et
71 al. 2010). This is a non-parametric estimate for the dynamic probability-density function of a
72 random variable in space (in this case, the probability of meeting an infected precisely there) and is
73 usually employed for data smoothing on finite data samples. Applying the Density Kernel Estimator
74 Method, we obtain:

75
$$p_c(y) = \frac{1}{c h} \sum_{i=1}^c K\left(\frac{y-y_i}{h}\right) \quad (6).$$

76 Where $Y = \{y_i, i = 1, 2, \dots, c: y_i \in S\}$ is the sets of all points (the infected) in space S, (London); $y \in$
 77 S is the spatial variable K , smooth and symmetric, the kernel function for the probabilistic
 78 prediction model; h is the bandwidth parameter.

79

80 **3. Results**

81

82 *3.1. The dynamic probability-density risk-map for London*

83 We accessed the data published by the UK Government on the 1st of July 2020

84 (<https://coronavirus.data.gov.uk>). We used *Wolfram Mathematica* to develop the risk-map. The

85 software allowed obtaining Y_i points in London, each representing an infected, distributed through

86 the Montecarlo Method (Rubinstein and Kroese 2016) proportionally to the infects. The points

87 (infects) were distributed in the 33 areas of 0.2 grades (one for each borough). A smaller grade

88 value would have been mathematically possible yet meaningless in practice. A larger grade value

89 would have led, instead, to a rougher approximation. The 33 areas representing the 33 London's

90 boroughs were each centered on the geo-localization of s_i .

91 Table 1 reports the density probability for each Londoner attraction, with the normalized

92 probability's corresponding value. The higher the number associated with an attraction, the higher

93 the risk of meeting an infected there.

94

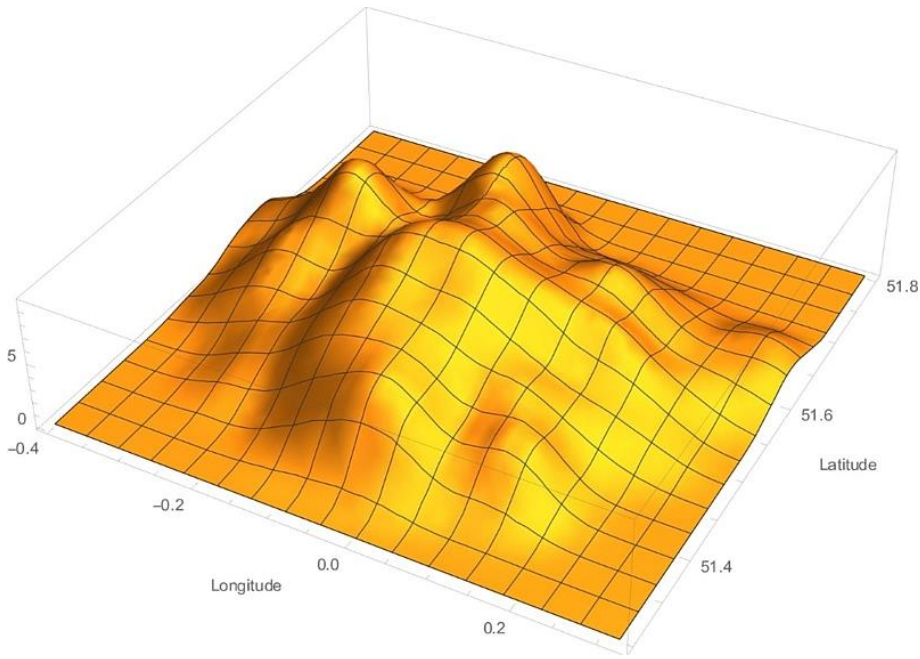
| Attraction | Normalized Risk value | Dynamic probability-density value |
|---------------------|-----------------------|-----------------------------------|
| National Gallery | 1.504262 | 7.702237 |
| Churchill War Rooms | 1.492284 | 7.400447 |
| St James's Park | 1.489627 | 7.33479 |
| British Museum | 1.529626 | 8.373883 |

| | | |
|-------------------------------|----------|----------|
| Victoria and Albert Museum | 1.450535 | 6,421557 |
| Tower Bridge | 1.519243 | 8.093494 |
| Tower of London | 1.525181 | 8.252911 |
| Westminster Abbey | 1.489354 | 7.328068 |
| Natural History Museum | 1.445969 | 6.321143 |
| Saint Paul's Cathedral | 1.534369 | 8.504517 |
| Royal Opera House | 1.517524 | 8.047818 |
| The Shard | 1.515375 | 7.990988 |
| London Eye | 1.500887 | 7.616228 |
| Hyde Park | 1.464095 | 6.727383 |
| House of Parliament | 1.490322 | 7.351912 |
| Borough Market | 1.517162 | 8.038224 |
| Sky Garden | 1.531034 | 8.412491 |
| Camden Market | 1.533886 | 8.491138 |

95 Table 1. Density probability for the main London attractions

96

97 Figure 1 shows the probability-density function $f(\phi)$, where the "peaks" and "valleys" represent -
98 respectively- a higher and lower probability of meeting infects. The three axes represent the latitude,
99 longitude, and probability of meeting an infect.



100

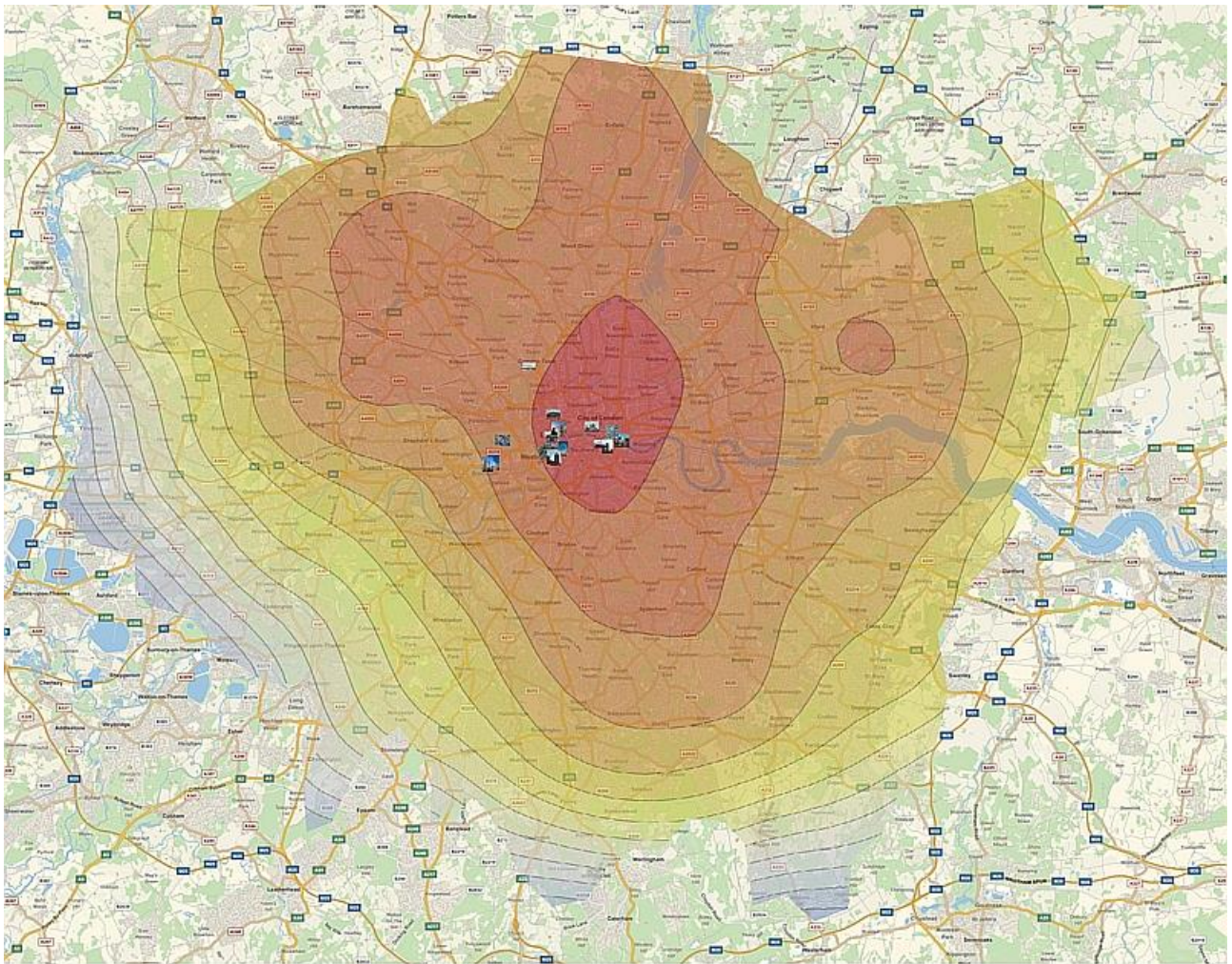
101 Figure 1: The dynamic probability-density function f .

102

103 Superimposing on Figure 1 the geographical map of London, we obtain the risk map in Figure 2. It
104 can be zoomed in/out at will. Risk is shown with colors, from blue (lowest) to red (highest) instead
105 of peaks.

106

107 Figure 2: London dynamic probability-density risk-map for COVID-19 contagion (July 2020).



108

109

110 *3.2 Tourists' reaction to the risk-map*

111 We run an online survey on 200 prospective Italian tourists (50% females, mean age = 25) from a
 112 Market Research company. Italy was the first country in Europe to lift travel restrictions, and about
 113 2.50 million Italians yearly visit London, according to the UK National Tourism Agency.

114 Respondents saw either a normal geographical map or the risk map (randomized between-subjects).
 115 Both maps were 30cmx30cm (11x11 inches) with 300dpi resolution and could be explored (scrolling
 116 and zooming in/out). Respondents stated their perceived risk of traveling to London and travel
 117 intention in the near future. Then, they all saw the risk-map and stated their attitude toward the risk-
 118 map and perceived usefulness.

119 The risk map significantly lowered risk perception ($\text{Mean}_{\text{normal-map}} = 4.83$ vs. $\text{Mean}_{\text{risk-map}} = 3.48$; $F =$
120 $54.63(1, 191)$, $p < .001$) and heightened travel intention ($\text{Mean}_{\text{normal-map}} = 3.13$ vs. $\text{Mean}_{\text{risk-map}} = 4.20$;
121 $F = 16.21(1, 191)$, $p < .001$). Perceived usefulness and attitude toward the map scored high
122 (Usefulness: Mean = 5.10 St.Dev = 1.72, Median = 5.00; Attitude: Mean = 5.17, St.dev = 1.55,
123 Median = 5.30).

124 In-depth, semi-structured interviews were run on with randomly extracted respondents with an
125 introspective approach to explore reactions to the map, following McCracken (1988). They quickly
126 converged after 20 interviews. Respondents revealed they opted for close rather than international
127 destinations due to a lack of such information to minimize contagion risk. They stated the risk-map
128 did not make them rule out traveling to London, and suggested them to avoid those attractions that
129 were in boroughs at risk of contagion.

130 Overall, this example shows that the map influences respondents, supporting their decision-making.

131

132 **4. Conclusion**

133 This research provides a new procedure to map risk. The results lead to a high-resolution, extremely
134 detailed map, where tourists' attractions are mapped together with the dynamic probability-density
135 function of being exposed to health risks. These risk map apply to anyone visiting the region, and to
136 residents, but are of particular interest for tourists, as they allow plotting risk-levels on a
137 geographical map while highlighting specific landmarks, like tourist attractions (as shown in figure
138 2), and associate them with the punctual probability of contagion.

139 These maps can contribute to the research on COVID-19 effects on the tourism industry (Karabulut
140 et al. 2020; Zenker and Kock 2020), and can also be applied to different risks (i.e., other diseases,
141 terrorism, etc.). They show that, even where the overall risk is high, risk can change from area to area
142 and from time to time. Thus, they allow enforcing safe routes for tourists, rather than shutting the
143 whole area down. Especially for those areas with high income from tourism, this would greatly impact
144 the local tourism industry's survival by avoiding tourism bans and closure of all attractions.

145 In a nutshell, the use of dynamic probability-density risk-maps can be framed in the broader topic of
146 technology helping tourism destinations (Park, 2000), represent a predictive model to formulate
147 new tourism scenarios, and answer recent calls for new tools to protect tourists against health risks
148 (Wang et al. 2019; Wolff et al. 2019).

149

150 REFERENCES

151 Bertacchini, F., Bilotta, E., & Pantano, P.S. (2020). On the temporal spreading of the SARS-CoV-2.
152 *PLoS ONE* 15(10), e0240777.

153 Botev, Z.I., Grotowski, J.F., & Kroese, D.P. (2010). Kernel density estimation via diffusion. *Annals*
154 *of Statistics* 38(5), 2916-2957.

155 Castorina, P., Iorio, A., & Lanteri, D. (2020). Data analysis on Coronavirus spreading by
156 macroscopic growth laws. *International Journal of Modern Physics*, 31(07), 2050103.

157 Godio, A., Pace, F., & Vergnano, A. (2020). SEIR modeling of the Italian epidemic of SARS-CoV-
158 2 using computational swarm intelligence. *International Journal of Environmental Research*
159 *and Public Health*, 17(10), 3535.

160 Karabulut, G., Bilgin, M.H., Demir, E., & Doker, AC (2020). How pandemics affect tourism:
161 international evidence. *Annals of Tourism Research* 84: art. 102991.

162 McCracken, G. (1988). *The long interview*. Sage.

163 Park, S. (2020). Multifaced trust in tourism service robots. *Annals of Tourism Research*, 81,
164 102888.

165 Ritchie, B. W., & Jiang, Y. (2019). A review of research on tourism risk, crisis and disaster
166 management. *Annals of Tourism Research*, 79, 102812.

167 Rubinstein, R.Y., & Kroese, D.P. (2016). *Simulation and the Montecarlo Method*. UK: Wiley and
168 Sons.

- 169 Statista (2020). Number of overseas resident visits to London in 2019, by purpose of visit.
170 [https://www.statista.com/statistics/287958/number-of-global-visits-to-london-uk-by-purpose-
172 of-visit/](https://www.statista.com/statistics/287958/number-of-global-visits-to-london-uk-by-purpose-
171 of-visit/)
173 Wang, J., Liu-Lastres, B., Ritchie, B. W., & Mills, D. J. (2019). Travellers' self-protections against
174 health risks. *Annals of Tourism Research*, 78, 102743.
175 Wolff, K., Larsen, S., & Ogaard, T. (2019). How to define and measure risk perceptions. *Annals of
176 Tourism Research* 79, 102759.
177 Zenker, S., & Kock, F. (2020). The coronavirus pandemic- A critical discussion of a tourism
178 research agenda. *Tourism Management*, 81, 104164.